A Two-Phase Three-Wire Quasi-Z-Source based Railway Power Quality Compensator for AC Rail Networks

Hamed Jafari Kaleybar*, Hossein Madadi Kojabadi
Department of Electrical Engineering
Sahand University of Technology
Tabriz, Iran
jafarik.hamed@gmail.com
hmadadi64@yahoo.ca

Morris Brenna, Federica Foiadelli
Department of Energy
Polytechnic University of Milan
Milan, Italy
morris.brenna@polimi.it
federica.foiadelli@polimi.it

Seyed Saeed Fazel
School of Railway Engineering
Iran University of Science and Technology
Tehran, Iran
fazel@iust.ac.ir

***Abstract*—Power quality (PQ) problems of AC railway systems have become a major obstacle so that over the years different compensation methods have been introduced to dominate them. Railway Power Quality Compensator (RPQC) is one of the effective strategies which had been presented with different structures and compensation methods. However, these conditioners basically have high capacity and also high potential to be exposed to destruction due to the shoot-through switching. In this paper a quasi Z-source based Railway Power Quality Compensator (qZRPQC) is proposed to improve mentioned problems. The proposed configuration is based on two-phase, three-wire converter composed of two step-down transformers connected to the two adjacent sections of the traction power substation. Despite having the all features of traditional RPQC, the proposed configuration can decrease the rating of the converter and increase the efficiency and reliability. In order to verify the performance and effectiveness of the proposed strategy the precise simulation results have been provided.**

Keywords—power quality; AC railway network; quasi Z-source converter; traction power substation

I. INTRODUCTION

Single-phase 25 kV AC power supply system is being widely adopted in rail networks around the world. The power quality problems of such a network in the local and upstream grid are one of the main concerns of experts [1-3]. Due to the using of single-phase supply, the railway system generates a large amount of negative sequence components (NSC) to the public grid. These NSC can lead to additional loss, overheating of motors and transformers, undesired tripping and failure of relays [4, 5]. On the other side, the wide spectrum of harmonics is also generated by traction motor drives, pantograph sliding contact uninterruptible power supply for the feeding of on-board auxiliary services and etc., which may lead to torque pulses and drops of rotating machines, interface with the signaling systems, communication devices additional temperature rise of equipment, vibrations of power capacitor banks and protective systems [6, 7]. In fact, due to the high-power and high-capacity trains of high-speed railway (HSR), research and concentration on RPQC has been increased significantly. In recent years, numerous researches have accomplished about different aspects of RPQC containing, configuration, compensation strategies and control system [8-10]. Despite the fact that the power rating and efficiency of RPQC is substantially important, the number of articles regarding to this area, is limited. In [11] a Hybrid Power Quality Compensator was introduced in order to decrease the operating voltage level and the rating of compensator. But, the low operating voltage reduces the system efficiency compensating performance. A simplified half-bridge based back-to-back converter is presented in [12] which leads to a decreased number of power switch in RPQC. However, reduction in the switch number increases the voltage and current stress over switches. In addition, this topology formed by two DC-link capacitors in series, which lead to the complex and difficult DC-link voltage control system. Adopting TSC along with RPQC and parallel with feeders was proposed in [13] to reduce the power rating. It should be pointed that using TSC can generate a wide spectrum of harmonics and cause additional installation costs. Beside all the restrictions mentioned, all of the introduced structures for RPQC are based on Voltage-Source Converter (VSC). The VSC acts as a buck converter in inversion mode and boost converter in rectification mode. Due to the fact that, the RPQC works in both modes, the operational DC-link voltage and capacitor rating together with the rating of whole converter should be high enough. In [14] a traditional Z-Source Converter (ZSC) is used in configuration of railway compensator in order to benefit its advantages. However, the voltage fed ZSC has some substantial drawbacks such as the input current is discontinuous and the capacitors sustain a high voltage rating. Also, control of ZSC in a back-to-back configuration is a complex [15]. As a result, because of discontinuous input current, it is hard to control the DC-link voltage. Also, the employed capacitors in the configuration of compensator endure a high voltage. In addition, the power transferring in this topology is unidirectional. In this paper a new configuration of RPQC based on quasi Z-Source Converter (qZSC) is proposed to overcome the mentioned limitations.

978-1-5386-3917-7/17/$31.00 ©2017 IEEE

The proposed topology is formed by qZSC together with two-phase, three-wire converter which is connected to the adjacent sections of Traction Power Substation (TPSS) through two step-down transformers. It can compensate all the important PQ indexes, including harmonics, NSC and low Power Factor (PF) simultaneously. The continuous current of DC-link capacitor in this qZSC makes this system suitable for railway power conditioning systems. The paper is structured as follows. In section II the proposed system details together with equivalent circuit are presented. Then in section III, the modified control strategy of qZRPQC has been studied in details. In section IV, the simulation results and analysis are presented and compared and finally, section V summarizes the paper and draws conclusions.

II. Principles of Proposed qZRPQC

A. Configuration

Fig.1 demonstrates the configuration of proposed qZRPQC in 1×25kV TPSS. The load currents in right and left sections (i_{LR}, i_{LL}) are forwarded to the traction motors through the overhead contact system and pantograph. In order to do the compensation duty such as compensate NSC, harmonic and reactive power completely, the primary side currents (i_A, i_B, i_C) should be completely sinusoidal, balanced in both phase and amplitude and also in the same phase of their voltages (V_A, V_B, V_C). Considering the three-phase to the two-phase traction transformer (known as balanced transformers) specifications used in TPSS, the secondary side currents of (i_R, i_L, i_G) are adjusted by injecting of the compensation currents (i_{rR}, i_{rL}, i_{rG}) through interface inductances (L_I) and step-down transformers. The phase diagram of TPSS voltages and currents is illustrated in Fig. 2. Regarding the type of traction transformer employed in TPSS and their secondary side connections, the currents in each section and the three-phase currents in primary side can be calculated as follows [16]:

$$\begin{cases} i_R = \dot{I}_a = \zeta_1 I e^{i(\theta_a-\varphi_a)} \\ i_L = \dot{I}_b = \zeta_2 I e^{i(\theta_a-\frac{\pi}{3}-\varphi_b)} \\ i_G = \dot{I}_c = -(\dot{I}_a+\dot{I}_b) = -I(\zeta_1 e^{i(\theta_a-\varphi_a)} + \zeta_2 e^{i(\theta_a-\frac{\pi}{3}-\varphi_b)}) \end{cases} \quad (1)$$

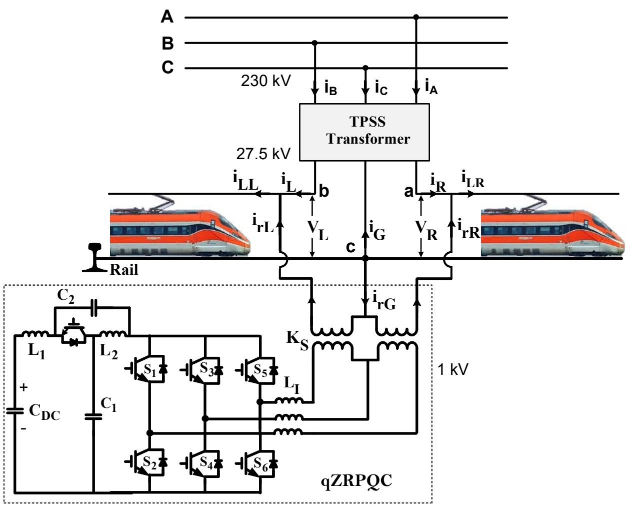

Fig. 1. Configuration of proposed qZRPQC in 1×25 kV–50 Hz TPSS

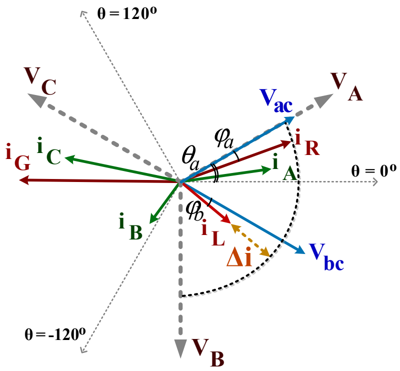

Fig. 2. Phase diagram of currents and voltages before compensation

$$\begin{bmatrix} i_A \\ i_B \\ i_C \end{bmatrix} = \frac{\sqrt{3}}{3a} \begin{bmatrix} I(2\zeta_1 e^{i(\theta_a-\varphi_a)} + \zeta_2 e^{i(\theta_a-\frac{\pi}{3}-\varphi_b)}) \\ \zeta_2 I e^{i(\theta_a-\frac{\pi}{3}-\varphi_b)} - \zeta_1 I e^{i(\theta_a-\varphi_a)} \\ -I(\zeta_1 e^{i(\theta_a-\varphi_a)} + 2\zeta_2 e^{i(\theta_a-\frac{\pi}{3}-\varphi_b)}) \end{bmatrix} \quad (2)$$

Where 'I' is the effective value of phase current, 'ζ' is the load balance ratios, 'θ_a' is the phase angle of $\dot{V}_A$ and 'φ_a' and 'φ_b' respectively are the phase difference of current and voltage in right and left sections. As seen in the figure, before compensation, the current amplitudes of the two sections are unbalanced and the primary side currents are asymmetrical too.

B. Equivalent Circuit and Operating Description

The equivalent circuit of the compensation system is shown in Fig. 3.a. Extracting the reference currents by modified control system, the proposed qZRPQC produces and injects the compensation currents to the system. In order to have a symmetrical qZSC the inductors L_1 and L_2 and capacitors C_1 and C_2 values are considered equal as L and C. The proposed qZSC has two working states. One is non shoot-through state illustrated in Fig. 3.b. In this case the qZSI operates as a traditional VSI and becomes an equivalent current source. The other one is the shoot-through state illustrated in Fig. 3.c. In this case the switches of at least one bridge leg are turned on. All the voltages and currents together with their polarities are defined in Fig. 3. Considering switching cycle as T_S, the period of the shoot-through state as T_{Sh} and the period of non-shoot-through states as T_1, the relations of switching cycle and shoot-through duty ratio can be written as:

$$\begin{cases} T_S = T_{Sh} + T_1 \\ D_{Sh} = {T_{Sh}}/{T_S} \\ 1 - D_{Sh} = {T_1}/{T_S} \end{cases} \quad (3)$$

During the non-shoot-through state the current flows from the Z-source network through the compensator inverter and single-phase transformers to the two adjacent sections of TPSS. As shown in Fig. 3.b it can be represented by an equivalent current source.

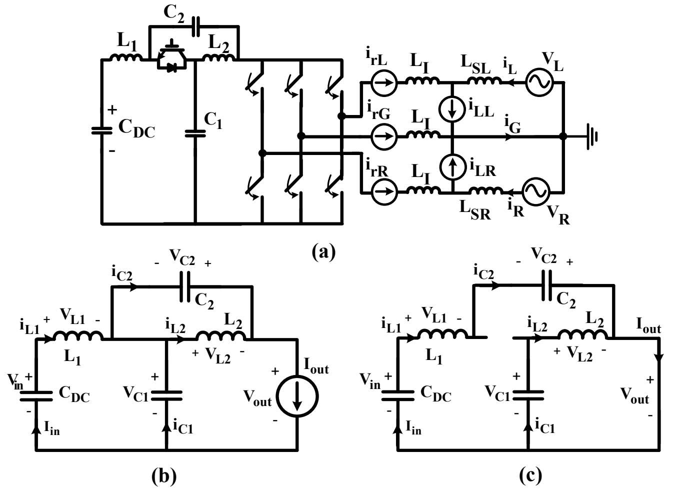

Fig. 3. Equivalent circuits. a) proposed compensation system b) qZRPQC non shoot-through state c) qZRPQC shoot-through state

The following equation can be calculated from this figure:

$$\begin{cases} V_{L_1} = V_{in} - V_{C_1} \\ V_{L_2} = -V_{C_2} \\ V_{out} = V_{C_1} - V_{L_1} = V_{C_1} + V_{C_2} \end{cases} \tag{4}$$

Where V_{in} is the DC-link voltage and V_{out} is the DC-link voltage across the inverter. In the shoot-through state the inverter side of qZRPQC is shorted. Fig. 3.c shows this state and following equation can be calculated:

$$\begin{cases} V_{L_1} = V_{C_2} + V_{in} \\ V_{L_2} = V_{C_2} \\ V_{out} = 0 \end{cases} \tag{5}$$

The inductor average voltage, over one switching cycle in steady state should be zero. Then:

$$\begin{cases} V_{L_1} = \bar{v}_{L1} = \dfrac{T_{Sh}(V_{C_2} + V_{in}) + T_1(V_{in} - V_{C_1})}{T_S} = 0 \\ V_{L_2} = \bar{v}_{L2} = \dfrac{T_{Sh}V_{C_1} + T_1(-V_{C_1})}{T_S} = 0 \end{cases} \tag{6}$$

$$\begin{cases} V_{C_1} = \dfrac{1 - D_{Sh}}{1 - 2D_{Sh}} V_{in} \\ V_{C_2} = \dfrac{D_{Sh}}{1 - 2D_{Sh}} V_{in} \end{cases} \tag{7}$$

The peak value of DC-link voltage across inverter can be calculated as:

$$\hat{V}_{out} = V_{C_1} + V_{C2} = \frac{1}{1 - 2D_{Sh}} V_{in} = \beta V_{in} \tag{8}$$

β is the boost factor of the qZSC. Using this boost specification, can decrease the capacity of DC-link voltage and capacitors. Considering M as modulation index, maximum ac output line to line voltage in qZRPQC can be written as follows:

$$\hat{V}_{ac} = M.B \frac{\hat{V}_{out}}{2} \tag{9}$$

III. CONTROL OF QZRPQC

In this part the modified control system for qZRPQC is presented. The proposed control system for qZRPQC composed of three main parts, including the reference current detection system, modulation strategy with the capability of shoot-through implementation and DC-link voltage controller.

A. Reference Current Detection Strategy

Due to the fact that, the secondary side connections of different transformers used in TPSS are not same, using control algorithm base on secondary side limits the performance of compensator. Therefore, in order to design a comprehensive control method and considering the difference between two main theories for implementing in proposed two phases system [17], a modified strategy based on Synchronous Reference Frame (SRF) is proposed. This method can be used for all kinds of TPSS transformers. As depicted in Fig. 4, using the Phase Locked Loop (PLL) and making π/2 lag in instantaneous voltages and currents, the obtained system can be represented in αβ -coordinate system as (10)-(11).

$$\begin{cases} \begin{pmatrix} V_{R\alpha}(t) \\ V_{R\beta}(t) \end{pmatrix} = \begin{pmatrix} \dot{V}_R(t) \\ \dot{V}'_R(t) \end{pmatrix} \\ \begin{pmatrix} V_{L\alpha}(t) \\ V_{L\beta}(t) \end{pmatrix} = \begin{pmatrix} \dot{V}_L(t) \\ \dot{V}'_L(t) \end{pmatrix} \end{cases} \tag{10}$$

$$\begin{cases} \begin{pmatrix} i_{R\alpha}(t) \\ i_{R\beta}(t) \end{pmatrix} = \begin{pmatrix} \dot{i}_R(t) \\ \dot{i}'_R(t) \end{pmatrix} \\ \begin{pmatrix} i_{L\alpha}(t) \\ i_{L\beta}(t) \end{pmatrix} = \begin{pmatrix} \dot{i}_L(t) \\ \dot{i}'_L(t) \end{pmatrix} \end{cases} \tag{11}$$

Where $\dot{V}'$ and $\dot{i}'$ are π/2 lag of voltages and currents. Implementing Park transformation, the currents in d-q frame can be calculated as:

$$\begin{pmatrix} i_{Rd}(t) \\ i_{Rq}(t) \end{pmatrix} = \begin{pmatrix} Cos\ \omega_R t & Sin\ \omega_R t \\ -Sin\ \omega_R t & Cos\ \omega_R t \end{pmatrix} \begin{pmatrix} i_{R\alpha}(t) \\ i_{R\beta}(t) \end{pmatrix} \tag{12}$$

$$\begin{pmatrix} i_{Ld}(t) \\ i_{Lq}(t) \end{pmatrix} = \begin{pmatrix} Cos\ \omega_L t & Sin\ \omega_L t \\ -Sin\ \omega_L t & Cos\ \omega_L t \end{pmatrix} \begin{pmatrix} i_{L\alpha}(t) \\ i_{L\beta}(t) \end{pmatrix} \tag{13}$$

Where, ω_R and ω_L are the right and left sections voltage angle.

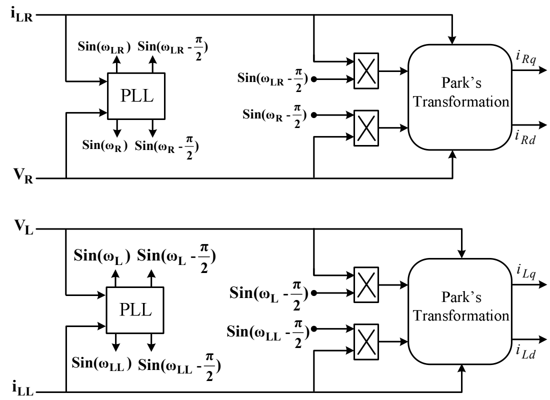

Fig. 4. Converting two-phases αβ-coordinate system to SRF.

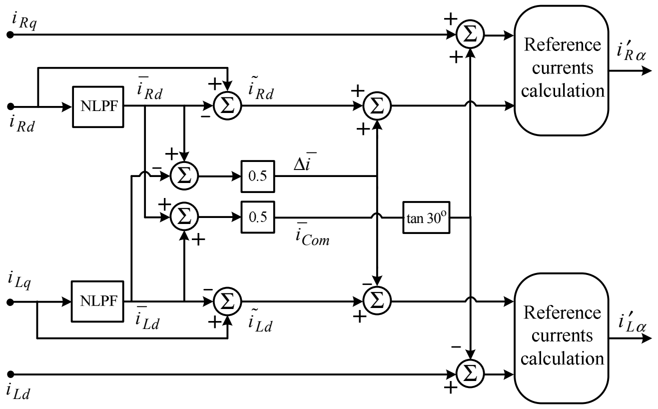

Fig. 5. Proposed SRF based control method block diagram

A numerical based low pass filter (NLPF) using variable forgetting factor recursive least squares (VFF-RLS) is implemented to separate dc parts and ac parts of currents [18]. In order to balance the currents, half of the fundamental current difference of the two sections should be transferred from the heavily-loaded section to the lightly-loaded section. Also, in order to compensate reactive power of the system caused by secondary connection of TPSS transformer, the common active power should be multiplied by a constant and added to the reactive powers [16]. The deferential and common currents of the two sections are as follows:

$$\begin{cases} \Delta\bar{i} = \dfrac{\bar{i}_{Rd}(t) - \bar{i}_{Ld}(t)}{2} \\ \bar{i}_{com}(t) = \dfrac{\bar{i}_{Rd}(t) + \bar{i}_{Ld}(t)}{2} \end{cases} \tag{14}$$

The required currents for producing the reference compensation currents can be calculated as:

$$\begin{pmatrix} i'_{Rd}(t) \\ i'_{Rq}(t) \\ i'_{Ld}(t) \\ i'_{Lq}(t) \end{pmatrix} = \begin{pmatrix} \tilde{i}_{Rd}(t) + \Delta\bar{i} \\ i_{Rq}(t) + (\frac{1}{\sqrt{3}}\bar{i}_{com}(t)) \\ \tilde{i}_{Ld}(t) - \Delta\bar{i} \\ i_{Lq}(t) - (\frac{1}{\sqrt{3}}\bar{i}_{com}(t)) \end{pmatrix} \tag{15}$$

Where, $\Delta\bar{i}$ is the difference of consumed fundamental current in two phases, $\tilde{i}_{Rd}(t)$ and $\tilde{i}_{Ld}(t)$ are the ac parts of right and left sections currents in d axis. Similarly, i_{Rq} and i_{Lq} are the reactive components in q axis. The primary reference compensating currents can be calculated using the reverse Park's transformation.

$$\begin{pmatrix} i'_{R\alpha}(t) \\ i'_{R\beta}(t) \end{pmatrix} = \begin{pmatrix} Cos\ \omega_R t & Sin\ \omega_R t \\ -Sin\ \omega_R t & Cos\ \omega_R t \end{pmatrix}^{-1} \begin{pmatrix} i'_{Rd}(t) \\ i'_{Rq}(t) \end{pmatrix} \tag{16}$$

$$\begin{pmatrix} i'_{L\alpha}(t) \\ i'_{L\beta}(t) \end{pmatrix} = \begin{pmatrix} Cos\ \omega_L t & Sin\ \omega_L t \\ -Sin\ \omega_L t & Cos\ \omega_L t \end{pmatrix}^{-1} \begin{pmatrix} i'_{Ld}(t) \\ i'_{Lq}(t) \end{pmatrix} \tag{17}$$

The block diagram of proposed SRF based control strategy is illustrated in Fig. 5. The primary output reference currents are forwarded to the further controller section which is depicted in Fig. 6. This section will be explained in next section.

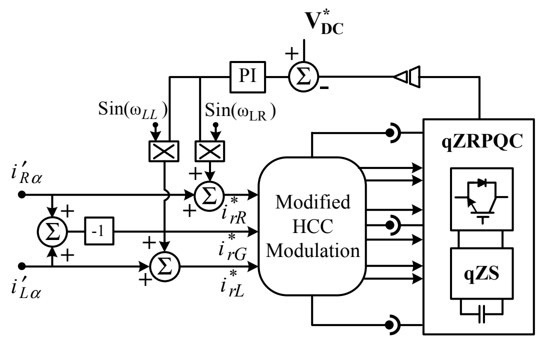

Fig. 6. Voltage controller and modulation technique block diagram

B. Current Control based Modulation System

Many PWM techniques together with special space vector modulation have been presented with embedded shoot-trough state [19, 20]. The main drawback of these techniques is the high demands to the complex control system. On the other side, due to the fast dynamic of traction system, there is a need for a fast and accurate control system. Hysteresis current control (HCC) technique is basically an instantaneous feedback current control of PWM where, the actual current continually tracks the reference current within a hysteresis band. The HCC PWM technique is well known because of the excellent dynamic response, simplicity, fast deadbeat transient response, high accuracy with minimum hardware and overcurrent protection [21]. However, it is difficult to implement it in a conventional format considering shoot-through states. In this case, a modified three modes HCC technique with distributed shoot-through states is proposed. The modified HCC PWM technique is set as upper and lower hysteresis band h and an interval band δ called shoot-through zone as shown in Fig. 7. When the actual current reaches the upper band the zero state is switched on. Therefore, the actual current forced to reverse direction. As soon as the actual current crosses the shoot-through band, the shoot-through state is switched on.

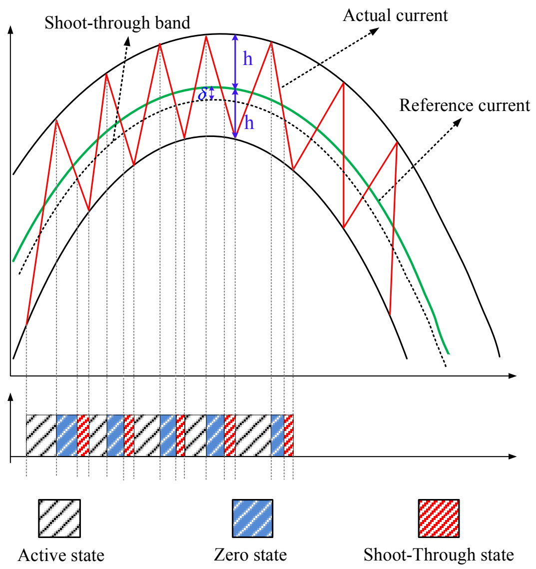

Fig. 7. Currents tracking in modified hysteresis PWM modulation technique

TABLE I. SWITCHING PATTERNS OF PROPOSED QZRPQC

Operation Mode	**Switching states**					
	S_1	S_2	S_3	S_4	S_5	S_6
Non Shoot-through	1	0	0	0	0	1
	1	0	1	0	0	0
	0	0	1	0	1	0
	0	1	0	0	1	0
	0	1	0	1	0	0
	0	0	0	1	0	1
Zero	1	0	1	0	1	0
	0	1	0	1	0	1
Shoot-through	1	1	S3	S3!	S5	S5!
	S1	S1	1	1	S5	S5!
	S1	S1!	S3	S3!	1	1
	1	1	1	1	S5	S5!
	1	1	S3	S3!	1	1
	S1	S1!	1	1	1	1
	1	1	1	1	1	1

Sx! is logical not of Sx. (*x=1, 3, 5*)

When the actual current reaches the lower band the active (non-shoot-through) state is started. Therefore, the actual current starts going up. The three-mode switching pattern is illustrated in Table I. All these states can be operated by proposed HCC method. Adjusting the band ratioes of h and δ, it can regulate the boost rating factor.

C. Voltage Controller

Regarding to qZRPQC topology and compensating of NSC, harmonic currents and reactive power, the DC-link capacitor voltage and output voltage of Z-source network should be stabilized to prepare an accurate performance of compensating. In order to reinstate this voltage, a conventional PI controller has been employed. This controller compares the reference voltage and measurement voltage and produces the proper signals to make the charging and discharging of capacitor balanced. As shown in Fig. 6, the final reference currents can be extracted as:

$$\begin{cases} i_{rR}^{*} = i'_{R\alpha} + i_{RS} \\ i_{rL}^{*} = i'_{L\alpha} + i_{LS} \\ i_{rG}^{*} = -(i_{rR}^{*} + i_{rL}^{*}) \end{cases} \quad (18)$$

Where, i_{RS} and i_{LS} are the stabilizing currents determined by PI controller.

IV. SIMULATION RESULTS

In order to validate the effective performance of the proposed configuration, simulations based on MATLAB/Simpower software have been carried out in two cases.

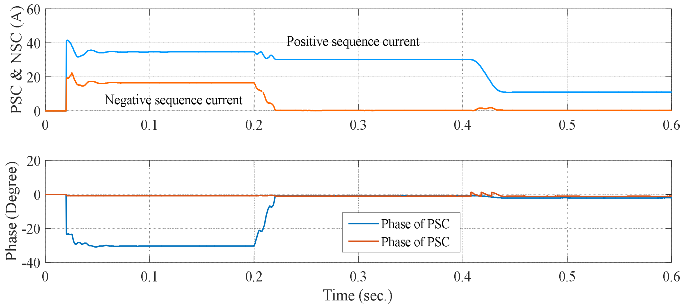

Fig. 8. Positive and negative sequence current in the grid-side

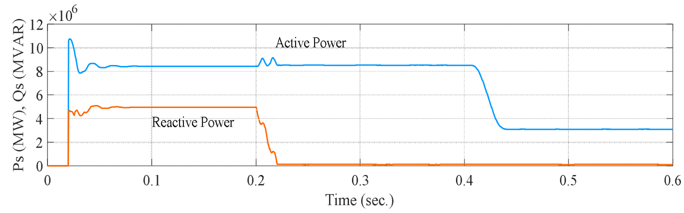

Fig. 9. Active and reactive power in grid-side

In case 1, there are two trains in both adjacent sections of TPSS with Load Balanced Ratio (LBR= 0.5). The power of train in right feeder (phase '*ac*') is 6 MW with PF of 0.86. In left feeder (phase '*bc*') the power is considered 3 MW with PF of 0.86. Due to the low power factor and harmonic characteristics of railway systems, traction load is modelled using a half controlled rectifier parallel with a resistance and inductance. The RPQC switched on at t= 0.2 s and compensation started. In case 2, at t= 0.4 s it is considered that the right section of the TPSS has no train and there is a train only in the left section (LBR=0). It can be seen from the simulation results shown that the Current Unbalanced Ratio (CUR), has been decreased so dramatically after using qZRPQC. The positive and negative sequence currents which are illustrated in Fig. 8 confirm this claim. In Fig. 9 active and reactive power of grid-side are shown. It is obvious that after starting of compensating the amount of reactive power consumed from the grid-side has been dropped to near zero. Therefore, the PF has improved from 0.86 to 0.99. As illustrated in Fig. 10, before compensation, the three-phase network-side currents are significantly unbalanced and overfilled of harmonic components. After compensation, the currents are getting sinusoidal and %THD has been reduced significantly in all cases. The phase currents and voltages of network-side are indicated in Fig. 11. The sinusoidal current waveforms after compensation are in the same phase of their voltages and PF had been improved.

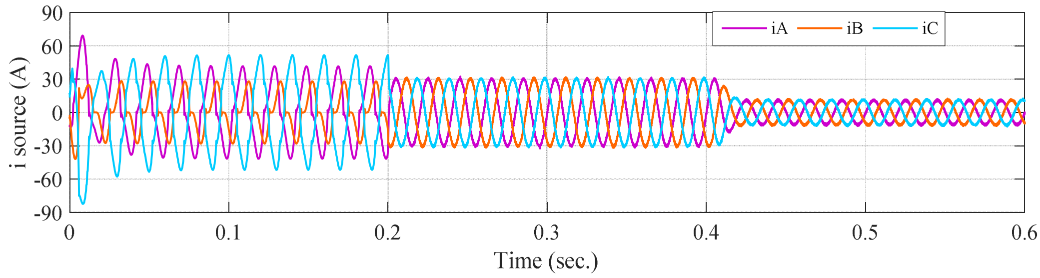

Fig. 10. Grid-side three-phase currents

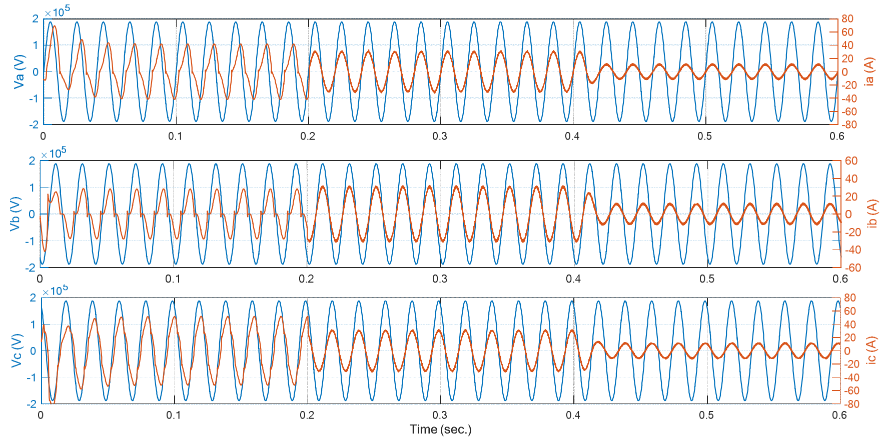

Fig. 11. Phase currents and voltages of network-side

V. Conclusion

In this paper, a new topology of railway power quality compensator has been presented to suppress harmonic currents, improve PF and eliminate NSC in TPSS. In the proposed configuration, adopting a qZSC together with a two-phase, three-wire converter leads the compensator as three controlled current source, which generate compensating reference currents through two step-down transformers and three switching inductances. A modified SRF based control strategy together with modified HCC is presented to control the proposed compensator. The qZRPQC has high capability to work with widely used traction transformers (V/V, Ynvd, Impedance matching). Due to the fast dynamic of railway systems, the analysis has investigated in two cases of load translocations. The precise simulation results verified the effective performance of the proposed strategy.

References

[1] P. Ladoux, J. Fabre and H. Caron, "Power Quality Improvement in ac Railway Substations: The concept of chopper-controlled impedance.," *IEEE Electrific. Mag.*, vol. 2, no. 3, pp. 6-15, Sept. 2014.

[2] M. Brenna, F. Foiadelli and D. Zaninelli, "Electromagnetic Model of High Speed Railway Lines for Power Quality Studies," *IEEE Trans. Power Syst.*, vol. 25, no. 3, pp. 1301-1308, Aug. 2010.

[3] G. D'Antona, R. Faranda, H. Hafezi, and M. Bugliesi, "Experiment on Bidirectional Single Phase Converter Applying Model Predictive Current Controller," *Energies*, vol. 9, no. 9, pp. 13, 24 Mar., 2016.

[4] B. Chen, C. Zhang, C. Tian, J. Wang and J. Yuan, "A Hybrid Electrical Magnetic Power Quality Compensation System With Minimum Active Compensation Capacity for V/V Cophase Railway Power Supply System," *IEEE Trans. Power Elec.*, vol. 31, no. 6, pp. 4159-4170, Jun. 2016.

[5] H. J. Kaleybar, S. Farshad, M. Asadi, and A. Jalilian, "Multifunctional control strategy of half-bridge based railway power quality conditioner for traction system," *in Proc. IEEE* 13th *Int. Conf. Environ. and Elec. Eng. (EEEIC)*, pp. 207–212, 2013.

[6] S. Hu *et al*., "A Power Factor-Oriented Railway Power Flow Controller for Power Quality Improvement in Electrical Railway Power System," in *IEEE Trans. Ind. Elec.*, vol. 64, no. 2, pp. 1167-1177, Feb. 2017.

[7] M. Brenna and F. Foiadelli, "Analysis of the Filters Installed in the Interconnection Points Between Different Railway Supply Systems," *IEEE Trans. Smart Grid*, vol. 3, no. 1, pp. 551-558, Mar. 2012.

[8] H. M. Kojabadi *et al*.,"Capacity diminution of railway power conditioner using a new smart control system," *in Proc. IEEE 8th Inter. Power Elec. and Motion Cont. Conf. (IPEMC-ECCE Asia)*, Hefei, 2016, pp. 2097-2102.

[9] A. Luo, F. Ma, C. Wu, S. Q. Ding, Q. C. Zhong and Z. Shuai, "A dualloop control strategy of railway static power regulator under V/V electric traction system," IEEE Trans. Power Elec., vol. 26, no. 7, pp. 2079– 2091, Jul. 2011.

[10] H. M. Kojabadi, H. J. Kaleybar, M. Fallah, S. S. Fazel and Liuchen Chang, "Capacity diminution of railway power conditioner using a new smart control system," *in Proc. IEEE 8th Inter. Power Elec. and Motion Control Conf. (IPEMC-ECCE Asia)*, Hefei, 2016, pp. 2097-2102.

[11] N. Y. Dai, K. W. Lao and C. S. Lam, "Hybrid Railway Power Conditioner With Partial Compensation for Converter Rating Reduction," *IEEE Trans.Ind. Appl.*, vol. 51, no. 5, pp. 4130-4138, Sept.-Oct. 2015.

[12] F. Ma, A. Luo, X. Xu, H. Xiao, Ch. Wu, W. Wang, "Simplified Power Conditioner Based on Half-Bridge Converter for High-Speed Railway System", *in Proc. IEEE Trans. Ind. Electron*., vol. 60, no. 2 , pp. 728–738, Feb. 2013.

[13] Ghassemi, A., Fazel, S.S., Maghsoud, I. and Farshad, S., "Comprehensive study on the power rating of a railway power conditioner using thyristor switched capacitor", *IET Elec. Systems in Transport.* Vol. 4, no. 4, pp.97-106. Dec.2014.

[14] H. M. Roudsari, A. Jalilian and S. Jamali, "A Z-source railway static power conditioner for power quality improvement," *in Proc. IEEE 7th Power Elec. and Drive Sys. Tech. Conf. (PEDSTC)*, Tehran, 2016, pp. 261-267.

[15] J. Anderson and F.Z. Peng, "A Class of Quasi-Z-Source Inverters," *in Proc. IEEE Ind. App. Society Ann. Meeting,* 2008. *IAS* '08. , pp. 1-7, 5-9 Oct. 2008.

[16] H. J. Kaleybar, S. Farshad, "A comprehensive control strategy of railway power quality compensator for AC traction power supply systems," *Turk. J. Elec. Eng. & Comp. Sci*, vol. 24, no. 6, 4582-4603, 2016.

[17] H. Hafezi, E. Akpinar and A. Balikci, "Assessment of two different reactive power estimation methods on single phase loads," *in Proc. IEEE 16th Inter. Power Elec. and Motion Cont. Conf. and Expos.*, Antalya, 2014, pp. 82-87.

[18] H. J. Kaleybar *et al*., "A new robust dynamic control method for Railway Power Quality Compensator," *in Proc. IEEE 8th Inter. Power Elec. and Motion Cont. Conf. (IPEMC-ECCE Asia)*, Hefei, 2016, pp. 1345-1349.

[19] P. C. Loh, D. M. Vilathgamuwa, Y. S. Lai, G. T. Chua and Y. W. Li, "Pulse-width modulation of Zsource inverters," IEEE Trans. Power Elec., vol. 20, no. 6, pp. 1346-1355, Nov. 2005.

[20] M. Abarzadeh, H. F. Kivi and H. M. Kojabadi, "A modified SVM switching pattern for Z-source inverter," *in Proc. IEEE 7th Power Elec. and Drive Sys. Tech. Conf. (PEDSTC)*, Tehran, 2016, pp. 486-491.

[21] S. Buso, S. Fasolo, L. Malesani and P. Mattavelli, "A dead-beat adaptive hysteresis current control," *IEEE Trans. Ind. App.*, vol. 36, no. 4, pp. 1174-1180, Jul/Aug. 2000.